Homomorphic partial differential equation filtering method for electronic speckle pattern interferometry fringes based on fringe density

Fang Zhang (张 芳)[1,2*], Wenyao Liu (刘文耀)[1,2], Lin Xia (夏 琳)[1,2], Jinjiang Wang (王晋疆)[1,2], and Yue Zhu (朱 越)[1,2]

[1] *College of Precise Instrument and Optical Electronic Engineering, Tianjin University, Tianjin 300072*

[2] *Key Laboratory of Opto-Electronics Information Technical Science, Ministry of Education, Tianjin 300072*

[*] *E-mail: hhzhangfang@126.com*

Received July 1, 2008

Noise reduction is one of the most exciting problems in electronic speckle pattern interferometry. We present a homomorphic partial differential equation filtering method for interferometry fringe patterns. The diffusion speed of the equation is determined based on the fringe density. We test the new method on the computer-simulated fringe pattern and experimentally obtain the fringe pattern, and evaluate its filtering performance. The qualitative and quantitative analysis shows that this technique can filter off the additive and multiplicative noise of the fringe patterns effectively, and avoid blurring high-density fringe. It is more capable of improving the quality of fringe patterns than the classical filtering methods.

OCIS codes: 120.6160, 070.6110.

doi: 10.3788/COL20090703.0210.

Electronic speckle pattern interferometry (ESPI) is a well-known, nondestructive, and full-field technique for displacement measurements[1−3]. Accurate extraction of phase from fringe patterns is of fundamental importance for the successful application of ESPI in obtaining the displacement. However, the strong grain-shape random noise in fringe patterns leads to heavy restraint to phase extraction. Therefore, it is important to filter off the noise from fringe patterns to make phase extraction easier, more robust, and more accurate[2]. In general, the traditional filtering methods including spatial filtering and frequency filtering, usually result in blurring effect. Therefore, some algorithms have been proposed to reduce the noise for ESPI fringe patterns, including Lee filtering, which is a noise filtering by the use of local statistics[4], span filtering, which filters off the fringe noise in a curvature window[2], and recursive algorithm, which has high computation speed but the result has low contrast[5].

Since the initial evolving equation, heat conduction equation, was used in image filtering in 1983[6], various forms of partial differential equations (PDEs) have been proposed for the filtering of noisy images[7−12]. However, the existing PDE filtering methods usually lead to insufficient denoising in the interior area of fringe patterns, or blurring effect on the fringe patterns with high fringe density. This is because these general PDE methods do not consider the fringe features, i.e., the multiplicative noise and the fringe density.

Perona *et al.* proposed a nonlinear anisotropic diffusion equation (called PM equation)[7], which has been widely used in image denoising and enhancement. The gray levels of an image $u(x,y,t):\Omega\times[0,+\infty)\to R$ are diffused according to

$$\partial_t u = \operatorname{div}\left(c\left(|\nabla u|\right)\nabla u\right), \quad u\left(x,y,0\right)=I\left(x,y\right), \qquad (1)$$

where $I\left(x,y\right)$ is the initial image, ∇u is the gradient of u, and diffusion gene c is a nonincreasing function of the gradient such as $1/(1+|\nabla u|^2/k^2)$. It implies a direct relation between the image smoothness at a point and the image gradient[8]. Unfortunately, this model is very sensitive to noise.

By formally developing the divergence term, the PM equation can be described in the inner orthogonal coordinates based on the image feature[9]. We define the inner orthogonal coordinates, i.e., the normal direction $\vec{N}$ and the tangent direction $\vec{T}$ as

$$\vec{N}=(u_x,u_y)/\sqrt{u_x^2+u_y^2}, \quad \vec{T}=(-u_y,u_x)/\sqrt{u_x^2+u_y^2}. \qquad (2)$$

Then Eq. (1) can be put in terms of the second derivatives of $\vec{N}$ and $\vec{T}$:

$$\partial_t u = \frac{1}{1+|\nabla u|^2\Big/k^2}\left(\frac{1-|\nabla u|^2\Big/k^2}{1+|\nabla u|^2\Big/k^2}u_{NN}+u_{TT}\right), \qquad (3)$$

where

$$u_{NN}=\left(u_x^2u_{xx}+u_y^2u_{yy}+2u_xu_yu_{xy}\right)\Big/\left(u_x^2+u_y^2\right),$$

$$u_{TT}=\left(u_x^2u_{yy}+u_y^2u_{xx}-2u_xu_yu_{xy}\right)\Big/\left(u_x^2+u_y^2\right). \qquad (4)$$

From Eq. (3), one can find that if $|\nabla u|/k\le 1$, it is a forward diffusion model and the image becomes denoised; but if $|\nabla u|/k>1$, it includes a backward diffusion along the normal direction $\vec{N}$ and the equation is ill-posed in mathematics. Qian *et al.* modified the diffusion gene and proposed a new model[9]

$$\partial_t u = \frac{1}{\sqrt{1+|\nabla u|^2\Big/k^2}}\left(\frac{1}{1+|\nabla u|^2\Big/k^2}u_{NN}+u_{TT}\right), \qquad (5)$$

 © 2009 Chinese Optics Letters

which avoids the problem of backward diffusion.

In general, the intensity distribution of a noisy interferogram can be expressed as

$$I(x,y) = P(x,y) + Q(x,y) N_{\mathrm{m}}(x,y) \cos\varphi(x,y) + N_{\mathrm{A}}(x,y), \tag{6}$$

where $P(x,y)$ is the background, $Q(x,y)/P(x,y)$ is the fringe contrast, $N_{\mathrm{A}}(x,y)$ and $N_{\mathrm{m}}(x,y)$ are the additive noise and multiplicative noise of the fringe pattern, respectively. The phase $\varphi(x,y)$ is related to a physical variable to be inspected.

In this letter, we propose a homomorphic PDE filtering method for ESPI fringe patterns based on fringe features. Considering the feature of full of both additive noise and multiplicative noise in ESPI fringe patterns, we resort to the homomorphic PDE filtering algorithm[10]. This method firstly uses the PDE to filter off the additive noise of an image, then changes the image by logarithmic transform and applies the PM equation again to filter off the multiplicative noise, at last obtains the final denoised image by exponential transform.

As for the feature of different densities in the entire fringe pattern, the diffusion of the same degree is unreasonable and the fringe density must be considered in PDE filtering. Yang *et al.* proposed a simple and accurate accumulation method for the determination of the fringe density[13]. Firstly, define the differences along four certain orientations of 0°, 45°, 90°, and 135° as

$$\begin{aligned} d_0(i,j) &= |u_{i-1,j} - u_{i+1,j}| \times \sqrt{2}, \\ d_{45}(i,j) &= |u_{i-1,j+1} - u_{i+1,j-1}|, \\ d_{90}(i,j) &= |u_{i,j-1} - u_{i,j+1}| \times \sqrt{2}, \\ d_{135}(i,j) &= |u_{i-1,j-1} - u_{i+1,j+1}|, \end{aligned} \tag{7}$$

in which for any function (i.e., image) $u(x,y)$, we let $u_{i,j}$ denote $u(i,j)$ for $1 < i < M$, $1 < j < N$.

Secondly, calculate the four sums of differences along the four orientations in a $W \times W$ square window A as

$$D_{\mathrm{angle}}(i,j) = \sum_{(i,j)\in A} d_{\mathrm{angle}}(i,j), \quad (\mathrm{angle} = 0, 45, 90, 135). \tag{8}$$

Finally, the fringe number in the calculation window can be estimated with

$$D_n = \frac{1}{4BW}\left(|D_0 - D_{90}| + |D_{45} - D_{135}|\right). \tag{9}$$

In this letter, we choose B as a normalized coefficient, whose function is setting the values of D_n to $[0,1]$. In this way, the fringe density calculated at each point is recorded in a map $I_{\mathrm{d}}(x,y)$, namely fringe density map.

Using the obtained fringe density map $I_{\mathrm{d}}(x,y)$, we propose a new diffusion equation:

$$\partial_t u = \frac{(1 - qI_{\mathrm{d}})}{\sqrt{1 + |\nabla v|^2 / k^2}} \left(\frac{1}{1 + |\nabla v|^2 / k^2} u_{NN} + u_{TT} \right), \quad u(x,y,0) = I(x,y). \tag{10}$$

The term v is defined as $v = G_\sigma * u$, where $G_\sigma = C\sigma^{-1/2} \exp\left(\frac{-(x^2+y^2)}{4\sigma}\right)$ is a Gaussian smoothing kernel. The strong grain-shape random noises in ESPI fringe patterns always introduce very large oscillations of the gradient. To avoid noise-sensitive problem of the PM equation, Gaussian convolution is performed *a priori*.

Another term to be noted is the total diffusion gene $(1 - qI_{\mathrm{d}}) \Big/ \sqrt{1 + |\nabla v|^2 / k^2}$, which controls the diffusion speed of each pixel, with q being a constant between 0 and 1. The term of $1 \Big/ \sqrt{1 + |\nabla v|^2 / k^2}$ ensures the minimal diffusion at the edge of an image and $(1 - qI_{\mathrm{d}})$ guarantees less smooth in the area with high-density fringe than that with low-density fringe. Thanks for the previous Gaussian filter, the isolated noise, which has a large value of ∇u but small value of $\nabla(G_\sigma * u)$, will obtain the high diffusion speed; whereas, the true edge, which has a large value of $\nabla(G_\sigma * u)$, will gain low diffusion speed in the gradient direction and be preserved. In addition, owing to the normalized fringe density map I_{d}, the term of $(1 - qI_{\mathrm{d}})$, whose value is between $(1 - q)$ and 1, makes the total diffusion slower around the high-density fringe. And the function of q is balancing the diffusion speed between high-fringe-density area and low-fringe-density area.

We summarize the steps to implement the proposed homomorphic PDE filtering method as follows.

1) Establish the fringe density map $I_{\mathrm{d}}(x,y)$ for the initial ESPI fringe pattern $I(x,y)$ based on Eq. (9).

2) Using $I_{\mathrm{d}}(x,y)$, implement the PDE filtering Eq. (10) for $I(x,y)$ to filter off the additive noise, then map the gray value of the filtered result into [0,255], and obtain the mid-filtered image $I_1(x,y)$.

3) Transform $I_1(x,y)$ to $I_2(x,y)$ by

$$I_2(x,y) = 100 \lg\left[I_1(x,y) + 1\right], \tag{11}$$

where $I_1(x,y)$ is added by 1 and $\lg[I_1(x,y)+1]$ is multiplied by 100 to ensure $I_2(x,y)$ in [0,255].

4) Using $I_{\mathrm{d}}(x,y)$, implement Eq. (10) again to filter off the multiplicative noise and obtain the filtered image $I_3(x,y)$.

5) Transform $I_3(x,y)$ to $I_4(x,y)$ by

$$I_4(x,y) = 10^{\frac{1}{100} I_3(x,y)} \tag{12}$$

After mapping the gray values of $I_4(x,y)$ to [0,255], our final filtered result is acquired.

For performing our filtering methods numerically, we attempt to discretize them. We assume that the fringe density map I_{d} has been acquired. For any function (i.e., image) $u(x,y)$, we let $u_{i,j}$ denote $u(i,j)$, and $(I_{\mathrm{d}})_{i,j}$ denote $I_{\mathrm{d}}(i,j)$ for $1 \le i \le M$, $1 \le j \le N$. The evolution

equation obtains images at times $t_n = n\Delta t$. We denote $u(i,j,t_n)$ by $u^n_{i,j}$. The time derivative u_t at (i,j,t_n) is approximated by the forward difference

$$(u_t)^n_{i,j} = \left(u^{n+1}_{i,j} - u^n_{i,j}\right)/\Delta t, \tag{13}$$

where Δt is time step size. And the spatial derivatives are

$$\begin{aligned}
(u_x)^n_{i,j} &= \left(u^n_{i+1,j} - u^n_{i-1,j}\right)/2,\\
(u_y)^n_{i,j} &= \left(u^n_{i,j+1} - u^n_{i,j-1}\right)/2,\\
(u_{xx})^n_{i,j} &= u^n_{i+1,j} + u^n_{i-1,j} - 2u_{i,j},\\
(u_{yy})^n_{i,j} &= u^n_{i,j+1} + u^n_{i,j-1} - 2u_{i,j}.
\end{aligned} \tag{14}$$

And the boundary conditions are

$$\begin{aligned}
&u^n_{i,0} = u^n_{i,1},\ \ u^n_{i,N+1} = u^n_{i,N},\ \ i = 1,2,\cdots,M,\\
&u^n_{0,j} = u^n_{1,j},\ \ u^n_{M+1,j} = u^n_{M,j},\ \ j = 1,2,\cdots,N.
\end{aligned} \tag{15}$$

Then $(u_{NN})^n_{i,j}$ and $(u_{TT})^n_{i,j}$ can be calculated based on Eq. (4). We denote $\alpha^n_{i,j}$ as an approximation of $\left(1 + (|\nabla v|^n_{i,j})^2/k^2\right)^{-1/2}$, i.e.,

$$\begin{aligned}
&\alpha^n_{i,j}\\
&= \left(1 + \left[\left(\frac{v^n_{i,j+1} - v^n_{i,j-1}}{2}\right)^2 + \left(\frac{v^n_{i+1,j} - v^n_{i-1,j}}{2}\right)^2\right]/k^2\right)^{-1/2}.
\end{aligned} \tag{16}$$

Finally, we obtain the explicit discrete scheme of Eq. (10) as

$$\begin{aligned}
u^{n+1}_{i,j} &= u^n_{i,j}\\
&+\Delta t\alpha^n_{i,j}\left(1 - q\left(I_{\rm d}\right)^n_{i,j}\right)\left(\left(\alpha^n_{i,j}\right)^2\left(u_{NN}\right)^n_{i,j} + \left(u_{TT}\right)^n_{i,j}\right).
\end{aligned} \tag{17}$$

We have tested the proposed method on the computer-simulated fringes and experimentally obtained fringes, respectively, which include sparse and dense fringes. For presenting the real filtering performance of our homomorphic PDE, here the tested original speckle fringe patterns are also obtained by model (5) and the Lee filtering method.

Figure 1(a) shows a computer-simulated fringe generated based on Eq. (6) by $M \times N$ pixels with $N_{\rm m}(x,y)$ and $N_{\rm A}(x,y)$ uniformly distributed over the intervals $[0,1]$ and $[0, I_{\rm m}]$ respectively, where $I_{\rm m}$ is a constant value. Here, we choose $P(x,y) \equiv 150$, $Q(x,y) \equiv 100$, $I_{\rm m} = 50$, and $\varphi(x,y)$ is calculated from

$$\begin{aligned}
&\varphi(x,y) = 0.03\pi(x+y)\left[(x/M) + (y/N)\right],\\
&x = 1,2,\cdots,M, \quad y = 1,2,\cdots,N.
\end{aligned} \tag{18}$$

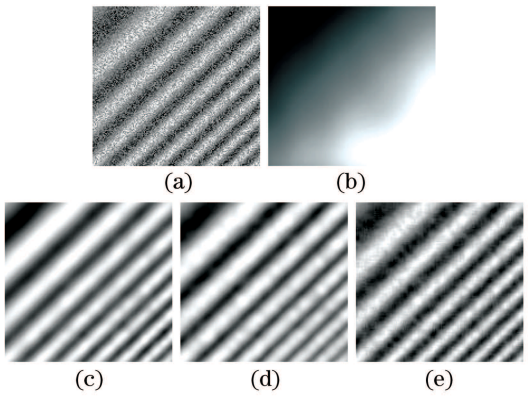

Fig. 1. A computer-simulated fringe pattern and its filtered images. (a) Initial image; (b) fringe density map; (c) our filtered image; (d) model (5) filtering image; (e) Lee filtering image.

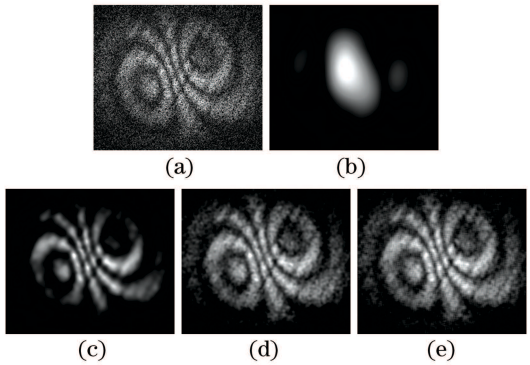

Fig. 2. An experimental fringe pattern and its filtered images. (a) Initial image; (b) fringe density map; (c) our filtered image; (d) model (5) filtering image; (e) Lee filtering image.

The fringe density values in Fig. 1(b) are represented by fringe numbers in a 51×51 square window. To avoid the inherent edge distortion error, we ignore 25 pixels at the boundary. In Fig. 1(b), the image gray denotes the fringe density. One can find that the lower gray values correspond to the lower fringe densities. Figure 1(c) is the filtered image by our method with several same parameters including $\Delta t = 0.2$, $k = 100$, $q = 0.8$ for the whole process, and different $n_1 = 20$ (i.e., 20 iterations) for filtering off the additive noise and $n_2 = 50$ for reducing the multiplicative noise. Figure 1(d) shows the result filtered by the model (5) with $\Delta t = 0.2$, $n = 20$, and $k = 100$. And the Lee filtering result is given in Fig. 1(e) in a 5×5 square window.

Figure 2(a) is an experimentally obtained fringe pattern, which depicts the derivative of the out-of-plane displacement of the side wall of a tire. Similar results for Fig. 2(a) as those for Fig. 1(a) are given in Figs. 2(b)—(e). The calculation window for fringe density map is also 51×51. The parameters for Figs. 2(c) and (d) are $\Delta t = 0.15$, $k = 100$, $q = 0.6$, and $n_1 = 8$ (filtering off the additive noise), $n_2 = 30$ (reducing the multiplicative noise), and $n = 8$ (denoising by model (5)), respectively. And a 5×5 square window is adopted in Lee filtering.

As we can see from the original images that the noise in the fringe patterns is high. It is noticed that the filtered fringes obtained by our method are smoother than those obtained by Lee filtering method (see Figs. 1(c), 1(e),

2(c), 2(e)), which indicates that our method can remove noise more effectively for the high-noise fringe patterns. Another obvious phenomenon is that the edges of the fringe patterns are better-preserved by our method than by the filtering model (5) (see Figs. 1(c), 1(d), 2(c), 2(d)), especially for Fig. 2(a), which has dense fringes.

To quantitatively evaluate the performance of our method further, the speckle index s[14] is used to quantify the local smoothness of the filtered fringe patterns. This parameter is evaluated as the average of the ratios of the local standard deviation to its mean:

$$s = \frac{1}{M \times N} \sum_{k=1}^{M} \sum_{l=1}^{N} \frac{\sigma_{k,l}}{\langle I_{k,l} \rangle}, \tag{19}$$

where $\langle I_{k,l} \rangle$ is the average gray in the neighborhood for a 3×3 window of the current point, and the local standard deviation $\sigma_{k,l}$ is defined as

$$\sigma_{k,l} = \sqrt{\frac{1}{8} \sum_{i=-1}^{1} \sum_{j=-1}^{1} (I_{k-i,l-j} - \langle I_{k,l} \rangle)}. \tag{20}$$

The speckle index can be regarded as an average reciprocal of signal-to-noise ratio (SNR), where the signal is the mean value and the noise is the standard deviation. Therefore, a low speckle index will be regarded as an indication of local smoothness of the fringe pattern.

We calculate the s values for the filtered results in Figs. 1 and 2, which are given in Table 1. The distinct results emerge from the analysis of the numerical tests. It can be seen that our method can give the lowest s among the three filtering methods for Figs. 1(a) and 2(a). The results are reasonable because our filtering method can filter off not only the additive noise but also the multiplicative noise. Meanwhile, our method can balance denoising and blurring by the density map, so that the noise area with low-density fringe can be smoothed sufficiently. Therefore, our filtering results are even better than those obtained by the other two methods.

Table 1. Performance Evaluation for the Three Filtering Methods

Image	Fig. 1			Fig. 2		
	(c)	(d)	(e)	(c)	(d)	(e)
s	0.1100	0.1123	0.1365	0.0873	0.0991	0.1101

In conclusion, we present an efficient homomorphic PDE filtering method based on fringe density for interferometric fringe patterns. First of all, the fringe density map is formed from the fringe pattern. Then, an improved homomorphic PDE filtering is implemented to filter off the additive and multiplicative noises of ESPI fringe patterns. This method can provide optimal results in denoising without destroying the fringe edges in excess, especially for dense fringes. We tested the proposed filtering method on computer-simulated and experimentally obtained ESPI fringe patterns respectively, and compared the results with the traditional filtering methods. The experimental results show that our method can provide good visual inspection and performance evaluation value. It is capable of significantly improving the quality of the fringe patterns.

References

1. S. Fu and Q. Yu, J. Appl. Opt. (in Chinese) **26,** (4) 5 (2005).
2. Q. Yu, X. Sun, X. Liu, and Z. Qiu, Appl. Opt. **41,** 2650 (2002).
3. J. Chen and Y. Hong, Acta Opt. Sin. (in Chinese) **24,** 1292 (2004).
4. J.-S. Lee, IEEE Trans. Pattern Anal. Machine Intell. **2,** 165 (1980).
5. Y. Qin, J. Chen, and H. Fan, Opt. Lasers Eng. **39,** 449 (2003).
6. A. P. Witkin, in *Proceedings of 8th Int. Joint Conf. Art. Intell.* 1019 (1983).
7. P. Perona and J. Malik, IEEE Trans. Pattern Anal. Machine Intell. **12,** 629 (1990).
8. G. Gilboa, N. Sochen, and Y. Y. Zeevi, IEEE Trans. Pattern Anal. Machine Intell. **26,** 1020 (2004).
9. W. Qian, R. Liu, W. Wang, S. Qi, W. Wang, and J. Cheng, J. Image Graphics (in Chinese) **11,** 818 (2006).
10. M. Xie and Z. Wang, Modern Radar (in Chinese) **27,** (9) 48 (2005).
11. F. Zhang, W. Liu, C. Tang, J. Wang, and L. Ren, Chin. Opt. Lett. **6,** 38 (2008).
12. F. Zhang, W. Liu, L. Li, L. Ren, and L. Yuan, Acta Opt. Sin. (in Chinese) **28,** 1475 (2008).
13. X. Yang, Q. Yu, and S. Fu, Opt. Commun. **274,** 286 (2007).
14. A. Dávila, G. H. Kaufmann, and D. Kerr, Opt. Eng. **35,** 3549 (1996).